A MECHANICAL APPROACH FOR THE MAXIMUM PUNCHING RESISTANCE OF SHEAR-REINFORCED SLAB-COLUMN CONNECTIONS

Diego Hernández Fraile [1, *], João T. Simões [2], Miguel Fernández Ruiz [3], Aurelio Muttoni [4]

[1]PhD Candidate, École Polytechnique Fédérale de Lausanne, 1015 Lausanne, Switzerland

[2]Structural Engineer, Strutlantis Engineering, Lisbon, Portugal, MFIC, Lausanne, Switzerland

[3]Senior Lecturer, École Polytechnique Fédérale de Lausanne, 1015 Lausanne, Switzerland

[4]Professor, École Polytechnique Fédérale de Lausanne, 1015 Lausanne, Switzerland

[*]Corresponding author email: diego.hernandezfraile@epfl.ch

Abstract

The use of punching shear reinforcement is currently considered as one of the most convenient practices to enhance the punching shear strength and deformation capacity of slab-column connections in flat slabs. Intensive research has been performed in the last decades on this topic, evidencing the complexity of the phenomenon, which is dependent on the anchorage conditions and detailing rules of the punching shear reinforcement, as well as on its capability to control cracking in the shear-critical region. Despite these efforts, the design of punching shear reinforcement, and particularly the verification of the maximum punching resistance, relies still on several empirical coefficients which enhance the calculated capacity of slabs without shear reinforcement. These methodologies require experimental validation, and no predictions or optimization can be performed on a scientific basis.

In an attempt to advance on a rational approach to the design of punching shear reinforcement, this paper introduces a novel methodology based on the fundamentals of the Critical Shear Crack Theory. By investigation of potential failure surfaces, the governing shape of the critical shear crack is determined and the contributions to the total resistance of concrete, flexural reinforcement and punching shear reinforcement are calculated accordingly (based on the slab rotations and the column penetration). This method is shown to be comprehensive and to consistently explain experimental evidence when compared to selected tests as well as general databases. The model is eventually used to show the role of a number of variables in the maximum punching strength behaviour of slab-column connections in flat slabs, including column size, detailing rules of punching reinforcement (spacing and anchorage performance), size effect and other parameters related to the level of strains in the slab (yield strength, amount of flexural reinforcement and slab slenderness).

Keywords: Critical Shear Crack Theory, flat slab, two-way shear, mechanical model, maximum punching strength.

1. Introduction

The punching failure of slab-column connections is a complex phenomenon whose understanding is still far for complete (*fib*-ACI (2017)). The resistance of members without shear reinforcement is in many cases governing at ultimate limit state and associated in general to low deformation capacities (Muttoni (2008)). One of the most efficient manners to enhance the response of slab-column connections has been identified as the addition of punching shear reinforcement, which allows increasing the resistance and deformation capacity at ultimate strength. Different punching shear reinforcement systems are currently available (Brantschen (2016), Einpaul et al. (2016)) showing a highly variable level of efficiency with

this respect. In particular, notable differences have been observed on the maximum punching shear capacity that can be attained, typically governed by the crushing resistance of the concrete near the column region, see Figure 1(c). The determination of this resistance, which is typically governing for choosing the slab thickness and the column size in the design phase, is normally considered with an empirically determined factor enhancing the punching strength of a slab without shear reinforcement (EN1992-1-1:2004 (EN 1992-1-1 (2004)), ACI 318-19 (2019)) or of its failure criterion (MC2010 (*fib* (2013)), CSCT (Muttoni (2008), Fernández Ruiz and Muttoni (2009))).

A deeper understanding of the phenomena governing the maximum punching shear resistance is however instrumental in order to avoid bias from experimental results (so that calibration of maximum punching resistance is not experimentally performed on the basis of favourable cases) and to conceive more efficient systems in the future. To that aim, supporting the performance of a punching shear reinforcing system on the basis of a mechanical model is a consistent manner to advance in this field. With this respect, this paper explores the suitability of the refined mechanical model developed by Simões, Fernández Ruiz and Muttoni (2018) based on the principles of the Critical Shear Crack Theory (CSCT (Muttoni (2008), Fernández Ruiz and Muttoni (2009))). As shown in this paper by means of comparisons of this model with available test results, the influence of a number of relevant parameters are captured, showing the deficiencies of current empirical calibrations. On this basis, a series of practical recommendations are proposed for the revision of EN 1992-1-1.

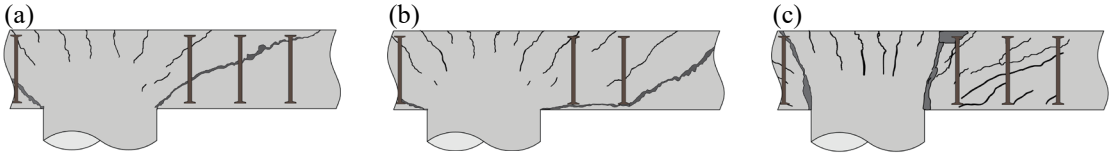

Figure 1. Punching failure modes in slab-column connections: failure within the shear-reinforced region (a), failure outside the shear-reinforced region (b), failure between the support and first perimeter of shear reinforcement (maximum punching failure) (c)

2. Mechanical model for punching of shear-reinforced connections

2.1. Origin and theoretical framework of the mechanical model

A refined mechanical model for punching shear failures of slab-column connections without shear reinforcement was developed and proposed by Simões, Fernández Ruiz and Muttoni (2018) based on experimental findings and the theoretical principles of the Critical Shear Crack Theory (Muttoni (2008)). This model allows determining the resistance and deformation capacity of a slab-column connection without shear reinforcement at failure. By imposing a given shape for the Critical Shear Crack (CSC) and a kinematics at failure (defined by means of the slab rotation and the shear deformations), the simplified analytical expressions originally proposed by the CSCT could be generalized. Notably, the influence of the shear deformations (penetration of column within the slab) could be accounted for in an explicit manner (independent from the slab rotations).

According to this refined model (Simões, Fernández Ruiz and Muttoni (2018)), the CSC is divided into two regions differentiated based on the kinematics at failure: a shear band developing smeared cracking in the bottom part and a localized crack behaviour in the upper part of the slab (Figure 2). In addition, dowelling of the hogging reinforcement can also be accounted for as a shear-carrying action. For each value of the slab rotation, the shear deformation that maximises the resistance of the connection can be found together with the governing kinematics at failure. The intersection of the curve resulting from the computation of the capacity for each level of slab rotation with a load-rotation relationship allows to find the resistance and kinematics (slab rotation and shear deformation) at failure of the connection; in this case the quadrilinear load-rotation relationship proposed by Muttoni (2008) is used. The general frame provided by this approach allows applying it to other cases, such as footings without shear reinforcement and prestressed slabs (Simões (2018)).

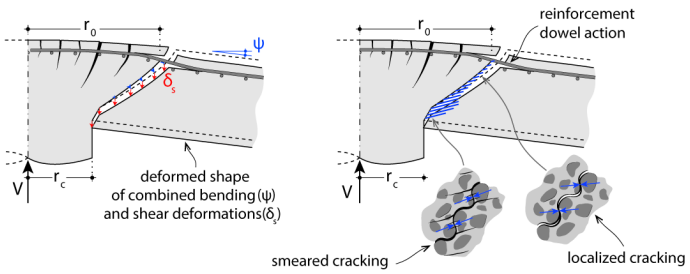

Figure 2. Kinematics and fundamentals of the mechanical model proposed by Simões, Fernández Ruiz and Muttoni (2018). Figure adapted from Simões, Fernández Ruiz and Muttoni (2018)

2.2. Model development for shear-reinforced slab-column connections

Based on these works, the model by Simões, Fernández Ruiz and Muttoni (2018) is extended in this manuscript to cover punching failures of shear-reinforced slab-column connections. This implies introducing a number of considerations:

- Consideration of an activation law for the shear reinforcement, determining the stress in the shear reinforcement when intercepted by the CSC as a function of two parameters -the height at which the CSC intercepts the reinforcement and the opening of the CSC at that same point- which are calculated based on the kinematics at failure and the assumed shape of the crack. The implemented activation law is the one proposed by Fernández Ruiz and Muttoni (2009), which showed to lead to consistent agreement with experimental observations (see extensions by Brantschen (2016)).
- Consideration of the position of the CSC at the level of the flexural reinforcement (defined as r_0, see Figures 2 and 3) into a fundamental variable, which is added to the slab rotations and shear deformations as a parameter for the calculation of the capacity of the connection. Under this assumption, the value of r_0 controls the failure mode, and allows reproducing both failures with activation of the punching reinforcement and by crushing of concrete struts (maximum punching failure), see Figure 1. Typically, for flatter inclinations of the CSC, see Figure 3(a), a higher amount of shear reinforcement can be activated, but this reduces the contribution of concrete to the overall strength. On the contrary, for steeper inclinations of the CSC, a lower amount of shear reinforcement is activated, but the contribution of concrete to the load-carrying capacity is higher. As a limit case, when no shear reinforcement is intercepted, all shear is carried by concrete, which ensures the maximum punching strength that can be transferred, see Figure 3(b).

As shown in Figure 3(c), for the slabs with shear reinforcement tested by Lips et al. (2012), a flatter crack inclination that activates two perimeters of shear reinforcement is expected up to a ratio of about 0.3%. For larger amounts of reinforcement, it becomes steeper, activating a single perimeter of reinforcement, which occurs until around 0.75%. For higher ratios, the maximum punching resistance is reached. The predictions of the model show good agreement with experimental observations on the shear strength and inclination of the failure surface (see Figure 3(c)). These results show a similar trend than those presented by Hoang and Pop (2016), with discrete vertical shifts in the curve as the number of punching reinforcement perimeters intercepted by the CSC changes as a function of its inclination.

In addition, the effect of the type of punching shear reinforcement can be explicitly considered, by implementing bond laws for the shear reinforcement as well as the performance of its anchorage (Brantschen (2016)). With this respect, one can distinguish in a rational manner between systems with anchoring conditions providing full anchorage (as studs), and systems with less performing anchorage conditions (as links, hooks and stirrups) (Fernández Ruiz and Muttoni (2009), Brantschen (2016), Einpaul et al. (2016)). The performance of the anchorage will be influenced by its geometric definition (size of the head or bent detail), detailing rules and by the cracked state of the slab (Brantschen (2016)). In order to consider also relatively steep cracks subjected to kinematics governed by large slips, the transfer of forces by rough surface contact and aggregate interlock has been implemented according to

the detailed approach by Fernández Ruiz (2021), extending the validity of the law originally implemented by Simões et al. (2018) (based on the works by Cavagnis et al. (2018)).

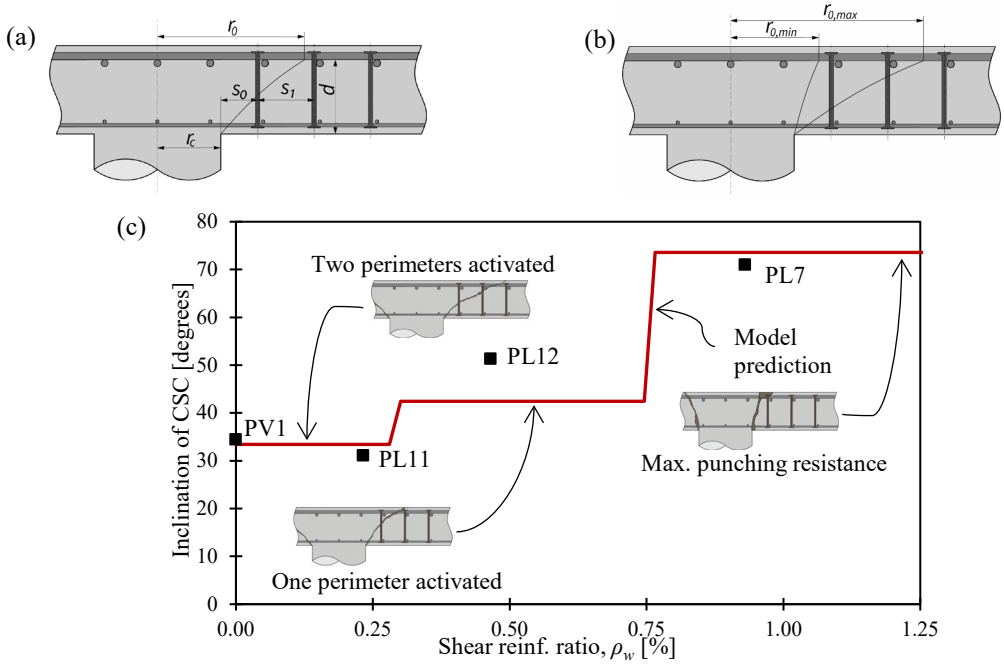

Figure 3. Definition of the mechanical model for shear-reinforced connections: fundamental parameters (a), representation of range of r_0 for shear-reinforced members (b) and variations of the inclination of CSC for increasing shear reinforcement ratios, predicted by the mechanical model and compared to measurements from experimental results (Lips et al. (2012))

2.3. Model validation and comparison with codes of practice

The suitability of the modifications implemented has been verified with available test data (Lips et al. (2012), Schmidt et al. (2020)). This has been done not only in terms of load and deformations at failure, but also of failure mechanisms. Selected comparisons are shown in Figure 4, together with predictions from several codes of practice, and from the analytical formulation of the Critical Shear Crack Theory (Muttoni (2008), Fernández Ruiz and Muttoni (2009)). The results show consistent agreement to tests, particularly enhancing the prediction of the strength for failures with activation of the shear reinforcement, contribution that codes of practice tend to underestimate. It is also notable the accurate prediction of the punching resistance irrespective of the type of shear reinforcement (studs or stirrups).

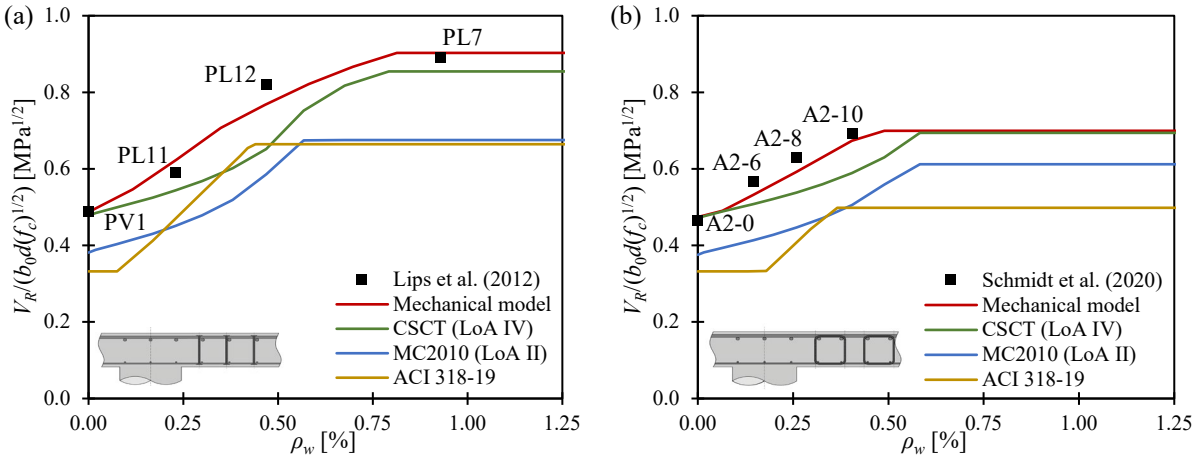

Figure 4. Results of punching shear resistance as function of the shear reinforcement ratio, considering the experimental results, mechanical model for shear-reinforced connections, and other predictions (ACI 318-19 (ACI 318 (2019)), Model Code 2010 (LoA II) (*fib* (2013)), and CSCT (Fernández Ruiz and Muttoni (2009))): series PV1/PL11/PL12/PL7 by Lips et al. (2012) (a) and A2-0/A2-6/A2-8/A2-10 by Schmidt et al. (2020) (b)

3. Influence on the maximum punching resistance of shear-reinforced slabs of geometric and mechanical parameters

The approach currently adopted by codes of practice follows typically an empirical calibration to determine the maximum punching shear strength. This is done multiplying the punching resistance of slabs without shear reinforcement or its failure criterion (as proposed by Model Code 2010) by a given factor. Such factor is normally determined for a specific punching reinforcement by comparison to test results and is typically assumed constant (independently of the geometry of the slab and the position of the shear reinforcement units, although they can vary). The performance of systems relies thus on the type of shear reinforcement used. For instance, the CSCT, on which Model Code 2010 is based (*fib* (2013)), proposes to increase the strength of the failure criterion of concrete by a factor 3 for studs, while it is only increased by 2.5 for stirrups (Fernández Ruiz and Muttoni (2009), Einpaul et al. (2016)) (the factors 3 and 2.5 correspond to approximatively 1.8 and 1.6 with respect to the increase of the resulting shear resistance). ACI 318-19 (ACI 318 (2019)) also accounts for this same differentiation by multiplying the resistance of a slab without shear reinforcement by a factor of 1.5 in the general case of shear-reinforced slabs, or by 2.0 in the case of double-headed studs. Following this trend, the new generation of Eurocode 2 (prEN 1992-1-1:2020-11 (2020)) also increases the shear strength of members without shear reinforcement by a coefficient named η_{sys} (equal to the ratio between the maximum punching strength of a slab with shear reinforcement and the strength of a slab without it). In the case of the maximum punching resistance calculations performed with Model Code 2010 (*fib* (2013)), there is no direct definition of η_{sys} in the code. However, for this paper and in order to make the results obtained with the different methods comparable, the maximum punching coefficient for Model Code 2010, η_{sysMC}, has been calculated as the ratio between the maximum punching resistance of the connection (computed with the failure criterion enhanced by the corresponding factor) and the punching resistance of the slab without shear reinforcement ($\eta_{sysMC}=V_{Rd,max}/V_{Rd,c}$).

With respect to the performance of the shear reinforcement, it shall be noted that the anchorage is not the only factor playing a relevant role in the maximum punching shear resistance of slabs, and the influence of other parameters has to be thoroughly analysed. This section presents the results of a parametric analysis performed with the refined model based on the CSCT and outlined in Section 2 to assess the maximum punching resistance of shear-reinforced slab-column connections. The results highlight the significance of several parameters and how they shall be considered for consistent and safe design.

3.1. Position of the first perimeter of shear reinforcement (s_0/d)

The position of the first perimeter of shear reinforcement (detailing rule) is an instrumental parameter, as it determines the inclination of the CSC controlling failures by crushing of concrete (and thus for maximum punching shear resistance). In general, for flatter angles of the CSC (occurring when the first perimeter of shear reinforcement is located farther away from the support region), the maximum punching resistance of the slab decreases. This effect was already observed by Einpaul et al. (2016) in experimental results, and has been confirmed with the mechanical model. Figure 5 shows with this respect the calculated influence of the distance between the column edge and the first perimeter of shear reinforcement (s_0, see Figure 3) on the maximum punching strength (expressed by means of η_{sys}). The calculated results according to the CSCT model confirm also the experimental trends observed by Einpaul et al. (2016) (Fig. 5(a)) , Gomes and Regan (1999) and Gomes and Andrade (2000) (Fig. 5(b)). This trend is not captured by Model Code 2010 or ACI 318-19, where the maximum punching resistance is independent of this parameter (with this respect, detailing rules in terms of maximum values of ratio s_0/d are defined to avoid cases with insufficient punching shear resistance). In particular, Model Code 2010 provides a good estimate for a position of the first perimeter quite close to the support region (s_0/d values between 0.3 and 0.4), while ACI 318 provides an unsafe estimate for both series of tests.

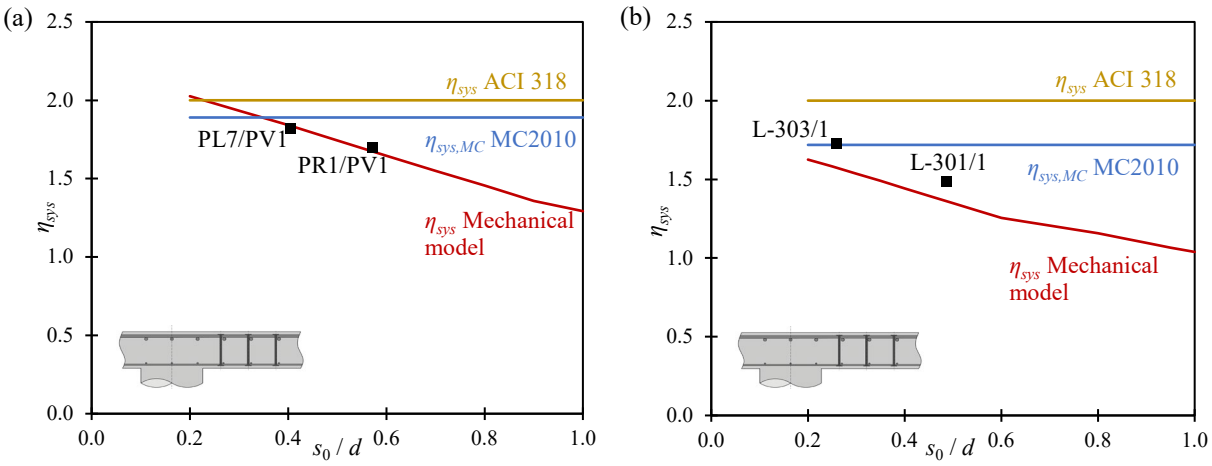

Figure 5. Effect of the position of the first perimeter of shear reinforcement in the maximum punching shear resistance of slabs: results presented in Einpaul et al. (2016) (a), and results gathered from Gomes and Regan (1999) and Gomes and Andrade (2000) (b)

3.2. Column size (r_c/d)

The size of the column has also been found to be a relevant parameter for the maximum punching failure. For small column sizes (values of r_c/d lower than 0.80, see Figure 3 for the definition of r_c), the value of η_{sys} decreases quite rapidly, with values approaching 1.0 for very small column sizes (r_c/d under 0.3), see for instance Figure 6. This implies that a much smaller enhancement on the strength and deformation capacity can be expected for these cases, even if equipped with shear reinforcement. In Figure 6, the results of the analyses performed are compared to the tests V4 and Z2 of Beutel (2002). For these tests, no reference specimens without punching shear reinforcement were available, so the reference values for the dots representing the tests have been calculated with the mechanical model as well. This figure shows that neglecting the ratio between the size of the column and the effective depth for the calculation of the maximum punching resistance coefficient of a slab could result in very unsafe estimates of the response (case of footings or situations with deep slabs for architectural purposes, thus having reduced column sizes). The predictions of ACI 318-19 do not depend of this parameter and are unsafe for small column sizes.

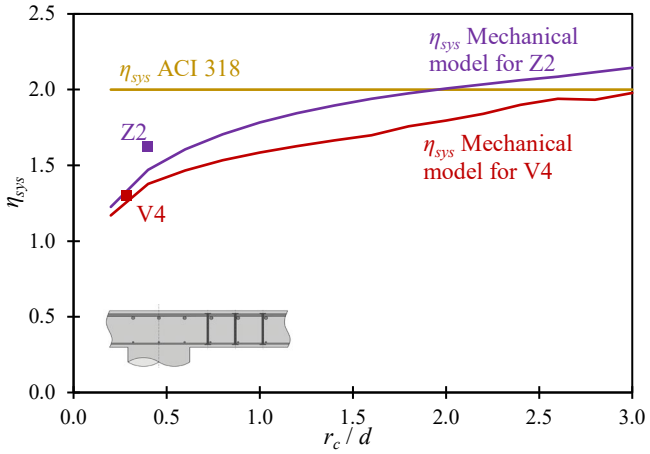

Figure 6. Effect of the column size in the maximum punching shear resistance of slabs. Tests in slabs with small column sizes relative to the slab depth, from Beutel (2002)

3.3. Flexural reinforcement: yield strength and reinforcement ratio

With respect to parameters influencing the flexural strength and thus the level of deformation in a slab, they are also observed to have a significant influence on the maximum punching resistance. As already demonstrated for slabs without punching shear reinforcement, lower crack widths (as those associated to higher values of the yield strength or of the reinforcement ratio) increase the capacity to transfer shear

stresses, due to a higher interlocking capacity (Fernández Ruiz (2021)), and thus the overall punching strength (Muttoni (2008)). This effect is also favourable with respect to the maximum punching shear strength, governed by the cracked concrete response, as shown in Figure 7(a) for the yield strength and Figure 7(b) for the reinforcement ratio. The formulation in Model Code 2010 captures the same trends observed in the mechanical model, with a very good fit for the variation of the flexural reinforcement ratio. However, ACI 318 formulation does not account for the influence of either flexural reinforcement parameter in the definition of the maximum punching resistance of a slab-column connection.

These influences are particularly relevant when constant values of η_{sys} are adopted for practical design based on comparison to tests. Such tests shall not be performed with too high flexural reinforcement ratios or with too high steel grades, as this might overestimate the actual strength in practical cases.

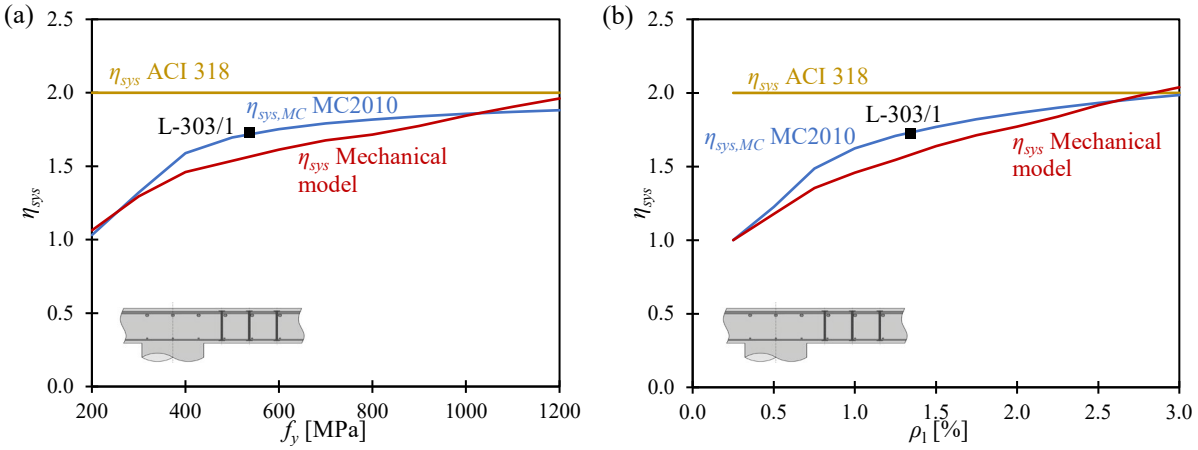

Figure 7. Effect of the yield strength of flexural reinforcement (a) and of the flexural reinforcement ratio (b) in the maximum punching resistance of slabs (Gomes and Regan (1999) and Gomes and Andrade (2000))

3.4. Slab geometry (effective depth and slab slenderness)

Finally, the effective depth of the slab (therefore analysing the importance of size effect) and its slenderness are also investigated. Both analyses are reflected in Figure 8. The ascending trend in the value of η_{sys} for increasing effective depths of the slab (Fig. 8(a)) is related to the fact that the size effect is milder for shear-reinforced slabs than for slabs without shear reinforcement, due to the higher level of load reached and to the higher degree of nonlinear response attained (Fernández Ruiz and Muttoni (2017)). With respect to the slab slenderness, Figure 8(b), it can be seen that it has a similar effect on slabs with and without shear reinforcement, therefore having limited influence on the maximum punching resistance coefficient, η_{sys}. The invariability of the predictions of ACI 318-19 is maintained for these two last parameters, with relatively unsafe results; Model Code 2010 shows a reduced variability, although there is a small influence of the size effect and the slab slenderness.

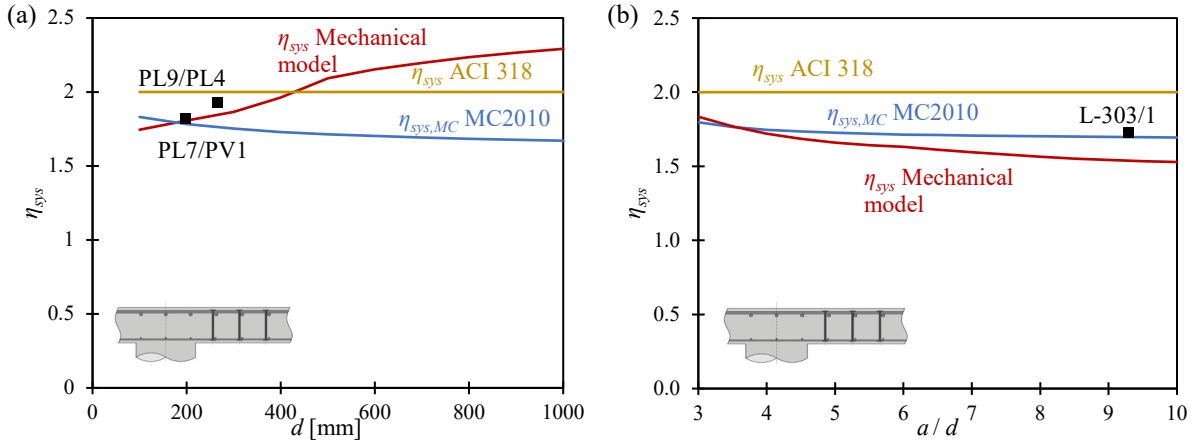

Figure 8. Effect of the effective depth of the slab (Lips et al. (2012)) (a) and of the slab slenderness (Gomes and Regan (1999) and Gomes and Andrade (2000)) (b) in the maximum punching resistance of slabs

4. Code-like proposal and comparison with current codes of practice

The parametric analyses performed with the mechanical model have allowed highlighting the most influential parameters on the maximum punching resistance of slab-column connections. As it can be noted, their influence might be significant and shall be accounted for to design these connections with a uniform level of safety.

Other than the performance of the anchorage, it is suggested to consider for a proper calculation of η_{sys} the influence of the position of the first perimeter of shear reinforcement and the ratio between the size of the column and the effective depth. For simplicity reasons, the following expression is proposed on the basis of the results of the mechanical model previously described (Sections 2-3):

$$\eta_{sys} = \frac{d_{sys}}{d_v} + 0.63\left(\frac{b_0}{d_v}\right)^{\frac{1}{4}} - \frac{s_0}{d_{sys}} \geq 1.0 \qquad (1)$$

where d_v is the effective depth of the slab, d_{sys} represents the height of the anchorage of the reinforcement system (thus well-anchored systems can have a ratio d_{sys}/d_v higher than 1.0), b_0 is the perimeter of the supported region, and s_0 is the distance from the column face to the axis of the first perimeter of shear reinforcement.

This expression is simple enough to be used for practical purposes and accounts for the influence of the main parameters involved. Figure 9 presents an example of comparison of the mechanical model predictions and the estimations with the proposed formulation. It relates to slab V4 from Beutel (2002), where significant deviations were observed with conventional approaches based on constant values of η_{sys} (refer to Figure 6). The value of d_{sys} was kept constant at the value calculated based on the definition of the slab; the ratio s_0/d_{sys} was varied; three column sizes were investigated, including the actual size of the tested specimen. The continuous curves correspond to the mechanical model calculations, the dashed curves to the formulation results, and the bullet to the test result; each colour corresponds to a different column size, indicated in Figure 9. It shows very good agreement between the mechanical model and the proposed Equation (1) for design, also in agreement with the test result.

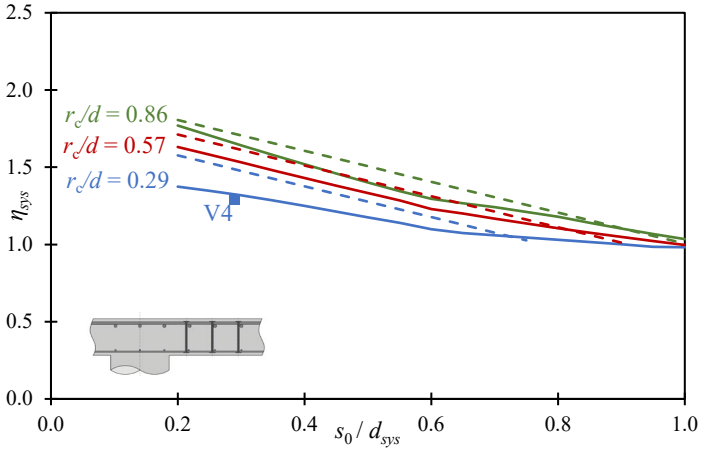

Figure 9. Comparison of the mechanical model predictions (in continuous lines) and the proposed Equation (1) (in dashed lines) for the slab geometry and reinforcement type of specimen V4 of Beutel (2002), for different column sizes relative to the effective depth, showing the influence of the position of the fist perimeter of shear reinforcement in the maximum punching coefficient η_{sys}

As it can be noted, the proposed Eq. (1) corresponds to a calibration to reproduce the predictions of the mechanical model. With respect to the different weights for each of the three factors involved, they can be tailored to the selected methodology for calculation of the punching resistance of slabs and to the purpose of use. Table 1 summarizes the proposed weights for different design purposes. The first one (same weights as Eq.(1)) relates to an accurate reproduction of the mechanical model. The second one minimizes the bias of the expression when compared to a database of test results (see Annex A). The third one ensures the same level of bias for tests with and without shear reinforcement when the design

model of prEN 1992-1-1:2020-11 (2020) is used for both cases (which corresponds to the actual definition for factor η_{sys}, Muttoni et al. (2021)).

Table 1. Weights given to the three factors of Equation (1) for three different purposes of use

Purpose of use	Reference for resistance of slab without punching reinforcement	Weight for d_{sys}/d_v	Weight for $(b_0/d_v)^{1/4}$	Weight for s_0/d_{sys}
Reproduction of mechanical model results	Mechanical model	1	0.63	1
Reproduction of experimental results (40 specimen database, see Annex A) with minimum bias (best fit to experiments)	prEN 1992-1-1:2020-11	1.15	0.63	0.85
Reproduction of experimental results (40 specimen database, see Annex A) with same bias as for slabs without punching reinforcement (Muttoni et al. (2021))	prEN 1992-1-1:2020-11	1.1	0.63	0.9

The comparison of the proposed Eq. (1), with weights adapted to keep the level of bias equal to punching design expressions of prEN 1992-1-1:2020-11 for slabs without shear reinforcement (i.e. as per the third row of Table 1, Muttoni et al. (2021)) against a database of 40 shear-reinforced slabs failing in maximum punching is presented in Figure 10. In the same figure, also the predictions of Model Code 2010 and ACI 318-19 are presented. The gathered database (see annex A) covers most slab and column geometries, flexural reinforcement ratios and shear reinforcement types and arrangements. In the figure, the vertical axis refers to the ratio between the experimental and the predicted failure load while the horizontal axis refers to the computed value of η_{sys}.

The results clearly show the necessity to incorporate for maximum punching design the influence of the various parameters discussed in order to lead to consistent results with low scatter. As can be seen from the statistical parameters (average value and coefficient of variation), the proposed formulation provides much better results than the provisions of ACI 318-19, which yields very conservative predictions with a relatively large scatter. Model Code 2010 provides a reasonable estimate on average, but with higher scatter.

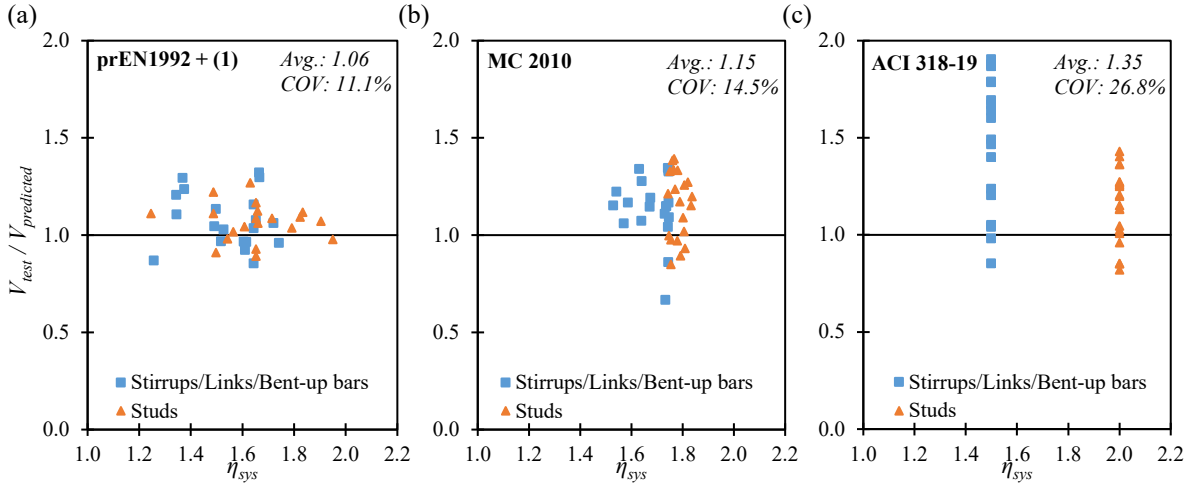

Figure 10. Accuracy of the proposed formulation compared to codes of practice: calculation of V_c as per prEN 1992-1-1:2020-11 (2020) and maximum punching coefficient as per proposed Equation (1) with weights as per last row of Table 1 (a); design calculation according to Model Code 2010 (Level of Approximation II) (b); design calculation according to ACI 318-19 (c)

5. Conclusions

This paper presents the results of an investigation on the maximum punching capacity of shear-reinforced slabs and the factors influencing it. Its main conclusions are summarized below:

1. The maximum punching resistance depends on the capacity of concrete to transfer shear forces between the column edge and the first perimeter of shear reinforcement. Thus, the inclination of the critical shear crack and its kinematics are governing. With this respect, the arrangement of the punching shear reinforcement and the performance of its anchorage are governing parameters controlling the shape of the critical shear crack and thus of the maximum punching resistance.
2. Other relevant parameters influencing the level of deformation of concrete play also a significant role, as the ratio between the column size and the effective depth or the amount of flexural reinforcement and its yield strength.
3. Consistent analyses of these phenomena can be performed on the basis of a refined implementation of the Critical Shear Crack Theory.
4. Empirical calibration of factors enhancing the punching strength of slabs without shear reinforcement can lead to unsafe estimates of the strength depending on the parameters selected for the reference tests.
5. Design for maximum punching shear resistance can be performed on the basis of simplified expressions accounting for the relevant parameters, such as anchorage performance and detailing, position of first perimeter of shear reinforcement and ratio between the column size and effective depth.

References

ACI 318 (2019). Building Code Requirements for Reinforced Concrete (ACI 318-19) - Farmington Hills, MI, USA.

Beutel R. (2002). Durchstanzen schubbewehrter Flachdecken im Bereich von Innenstützen - RWTH, Aachen, Germany, 267 p. (in German).

Brantschen F. (2016). Influence of Bond and Anchorage Conditions of the Shear Reinforcement on the Punching Strength of RC Slabs - PhD Thesis, ENAC-EPFL, Lausanne, Switzerland, 2016, 227p.

Cavagnis F, Fernández Ruiz M, Muttoni A. (2018). A Mechanical Model for Failures in Shear of Members Without Transverse Reinforcement Based on Development of a Critical Shear Crack – Eng. Struct. 2018, pp. 300-315.

Einpaul J., Brantschen F., Fernández Ruiz M., Muttoni A. (2016). Performance of Punching Shear Reinforcement Under Gravity Loading: Influence of Type and Detailing - ACI Structural Journal, Vol. 113, No. 4, Farmington Hills, USA, 2016, pp. 827-838.

EN 1992-1-1 (2004). Eurocode 2: Design of Concrete Structures—Part 1-1: General Rules and Rules for Buildings - CEN, Brussels, Belgium, 2004, 225 pp.

Etter S., Heinzmann D., Jäger T., Marti P (2009). Versuche zum Durchstanzverhalten von Stahlbetonplatten, IBK Bericht, 64, Zürich, Switzerland, December, 2009.

Feix J., Schustereder C. (2007). Durchstanzen nach EN 1992-1-1, Durchstanzversuche zur Festlegung der Nachweisgrenzen, Bauingenieur, vol. 82, pp. 135-142, Berlin, Germany

Fernández Ruiz M. (2021). The Influence of the Kinematics of Rough Surface Engagement on the Transfer of Forces in Cracked Concrete - Engineering Structures, 2021, 17 p.

Fernández Ruiz M., Muttoni A. (2017). Size Effect in Shear and Punching Shear Failures of Concrete Members Without Transverse Reinforcement: Differences Between Statically Determinate Members and Redundant Structures - Structural Concrete, 2017, 11p.

Fernández Ruiz M., Muttoni A. (2009). Applications of Critical Shear Crack Theory to Punching of Reinforced Concrete Slabs with Transverse Reinforcement - ACI Structural Journal, V. 106, No. 4, USA, 2009, pp. 485-494.

fib International Federation for Structural Concrete (2013). fib Model Code for Concrete Structures 2010 - Berlin: Ernst & Sohn, 2013; 434 pp.

fib-ACI (2017). Bulletin 81 / ACI SP-315: Punching shear of structural concrete slabs: Honoring Neil M. Hawkins. Tech. rep. Lausanne, Switzerland: International Federation for Structural Concrete, 378 p.

Gomes R.B., Andrade M.A.S. (2000). Does a Punching Shear Reinforcement Need to Embrace a Flexural Reinforcement of a RC Flat Slab? - International Workshop on Punching Shear Capacity of RC Slabs, Stockholm, Sweden, Jun. 2000, pp. 109-116.

Gomes R.B., Regan P.E. (1999). Punching Resistance of RC Flat Slabs with Shear Reinforcement - Journal of Structural Engineering, ASCE, V. 125, No. 6, 1999, pp. 684-692.

Hallgren M. (1996). Punching Shear Capacity of Reinforced High Strength Concrete Slabs, Doctoral thesis KTH Stockholm, Stockholm, Sweden.
Hoang, L.C., Pop, A. (2016). Punching shear capacity of reinforced concrete slabs with headed shear studs. Magazine of Concrete Research, 2016.
Ladner M. (1998). Durchstanzversuche an Flachdeckenausschnitten, Untersuchungsbericht 419, Hochschule Technik+Architektur Luzern, Materialprüfstelle der Abteilung Bau, Horw, Schweiz, 1998.
Lips S., Fernández Ruiz M., Muttoni A. (2012). Experimental Investigation on Punching Strength and Deformation Capacity of Shear-Reinforced Slabs - ACI Structural Journal, Vol. 109, USA, 2012, pp. 889-900.
Mueller F. X., Muttoni A., Thürlimann B. (1984). Durchstanzversuche an Flachdecken mit Aussparungen, IBK - Bericht (ETHZ), Institut für Baustatik und Konstruktion der ETH Zürich, Birkhäuser Verlag, 7305-5, 118 p., Zürich, Switzerland.
Muttoni A. (2008). Punching Shear Strength of Reinforced Concrete Slabs Without Transverse Reinforcement – ACI Structural Journal, V 105, No. 4, USA, 2008, pp. 440-450.
Muttoni A., Fernández Ruiz M., Simões J. T. (2018). The theoretical principles of the critical shear crack theory for punching shear failures and derivation of consistent closed-form design expressions, Structural Concrete, 2018, Vol. 19, pp. 174-190.
Muttoni A., Fernández Ruiz M., Simões J. T., Hernández Fraile D., Hegger J., Siburg C., and Kueres, D. (2021). prEN 1992-1-1:2020-11 Background document to Section 8.4 Punching, TG4-WG1-SC2-prEN 1992-1-1, CEN, 2021.
prEN 1992-1-1:2020-11 (2020). Eurocode 2: Design of concrete structures – Part 1-1: General rules – Rules for buildings, bridges and civil engineering structures (Draft version), WG1-CDG-prEN 1992-1-1, CEN, 2020.
Schmidt P., Kueres D., Hegger J. (2020). Punching Shear Behaviour of Reinforced Concrete Flat Slabs With a Varying Amount of Shear Reinforcement - Structural Concrete, 2020, 21, pp. 235-246.
Simões J. T., Fernández Ruiz M., Muttoni A. (2018). Validation of the Critical Shear Crack Theory for Punching of Slabs Without Transverse Reinforcement by Means of a Refined Mechanical Model - Structural Concrete, 2018, Vol. 19, pp. 191-216.
Simões J. T. (2018). The Mechanics of Punching in Reinforced Concrete Slabs and Footings Without Shear Reinforcement - PhD Thesis, ENAC-EPFL, Lausanne, Switzerland, 2018, 224p.
Yamada T., Nanni A., Endo K. (1992). Punching Shear Resistance of Flat Slabs: Influence of Reinforcement Type and Ratio, ACI Structural Journal, Vol. 88, pp. 555-563, Farmington Hills, USA.

Annex A

Table A shows a summary of the main parameters of the slabs that compose the database gathered for the analysis of the maximum punching resistance of slab-column connections presented in Section 4. All the specimens here presented are reported to have failed in maximum punching shear capacity.

Table A. Summary of specimens considered for the validation of the proposal

Reference	Specimen	B [m]	d [mm]	Column dimension [mm]	ρ_l [%]	f_y [MPa]	Shear reinforcement	ϕ_w [mm]	s_0 [mm]	ρ_w [%]	V_{test} [kN]
Mueller, Muttoni and Thürlimann (1984)	P22	2.75	154	300 (D)	1.31	551	Stirrups	8	49	0.70	1044
Yamada, Nanni and Endo (1992)	T4	2.00	167	300	1.33	811	Stirrups	13	64	0.97	697
	K2	2.00	164	300	1.54	568	Hooks	6	101	0.25	950
	K3	2.00	164	300	1.54	568	Hooks	6	99	0.50	1183
	K4	2.00	164	300	1.54	568	Hooks	10	101	0.55	1153
	K5	2.00	164	300	1.54	568	Hooks	10	97	1.11	1440
	K6	2.00	164	300	1.54	568	Hooks	13	101	0.99	1274
	K7	2.00	164	300	1.54	568	Hooks	13	97	1.98	1498
Hallgren (1996)	HSC3s	2.54	200	250 (D)	0.65	632	Bent-up Bars	16	124	-	1329
	HSC5s	2.54	201	250 (D)	1.03	604	Bent-up Bars	16	89	-	1631
	HSC7s	2.54	200	250 (D)	0.50	630	Bent-up Bars	16	124	-	1106

Reference	Specimen	B [m]	d [mm]	Column dimension [mm]	ρ_l [%]	f_y [MPa]	Shear reinforcement	ϕ_w [mm]	s_0 [mm]	ρ_w [%]	V_{test} [kN]
Ladner (1998)	2	3.30	240	300 (D)	1.31	510	Stirrups	10	111	0.93	1784
Gomes and Andrade (2000)	L-301	3.00	164	200	1.26	538	Stud rail	10	80	0.60	830
	L-302	3.00	164	200	1.26	538	Stud rail	10	40	1.19	790
	L-303	3.00	154	200	1.34	538	Stud rail	10	40	1.22	966
	L-308	3.00	154	200	1.34	538	Stud rail	13	40	1.27	1020
Beutel (2002)	P2-II	2.75	190	400	0.81	549	Stirrups	8	83	0.40	1145
	P4-III	2.75	222	320	1.13	557	Stirrups	8	114	0.66	1563
	V1	2.75	250	200 (D)	0.80	917	Headed Studs	16	88	0.57	1250
	V2	2.75	250	200 (D)	0.80	917	Headed Studs	16	113	0.57	1424
	V3	2.98	250	200 (D)	0.80	889	Headed Studs	16	88	0.57	1182
	V4	2.98	350	200 (D)	0.51	889	Headed Studs	16	131	0.44	1679
	Z1	2.98	250	200 (D)	0.80	889	Headed Studs	14	100	0.65	1323
	Z2	2.98	250	200 (D)	0.80	889	Headed Studs	14	88	0.65	1442
	Z3	2.98	250	200 (D)	0.80	889	Headed Studs	14	94	0.70	1616
	Z4	2.98	250	200 (D)	0.80	889	Headed Studs	14	88	0.75	1646
	Z5	2.98	250	263 (D)	1.26	562	Headed Studs	16	94	0.80	2024
	Z6	2.98	250	200 (D)	1.26	562	Headed Studs	16	94	0.91	1954
Feix and Schstereder (2007)	01-03	2.70	140	188.2 (D)	2.26	550	Stirrups	12	76	0.66	741
	01-04	2.70	135	188.2 (D)	2.34	550	Stirrups	12	76	0.67	717
	01-05	2.70	145	188.2 (D)	2.18	550	Stirrups	12	76	0.65	777
Hegger et al. (2007)	EM1	2.80	160	290	1.97	558	Stirrups	8	84	1.11	1213
Etter et al. (2009)	SP3	4.10	294	400 (D)	1.21	577	Headed Studs	18	93	0.93	3350
Lips et al. (2012)	PL6	3.00	198	130	1.59	583	Headed Studs	14	80	1.01	1363
	PL7	3.00	197	260	1.60	583	Headed Studs	14	80	0.93	1773
	PL9	3.00	266	340	1.59	562	Headed Studs	18	100	0.93	3132
	PF2	3.00	208	260	1.51	583	Stirrups	10	131	0.79	1567
Einpaul et al. (2016)	PB3	3.00	205	260	1.54	576	Links	10	131	0.79	1697
	PR1	3.00	210	260	1.50	515	Headed Studs	14	120	1.04	1654
	PE1	3.00	200	260	1.57	590	Headed Studs	16	80	0.92	1857

Note: B corresponds to the longest dimension of the slab specimen; d is the effective depth of the slab; *column dimension* corresponds to the side length of a square column unless *(D)* is indicated, meaning that the column dimension corresponds to the column diameter; ρ_l is the flexural reinforcement ratio; f_y is the yield strength of the flexural reinforcement; ϕ_w is the diameter of the punching shear reinforcement; s_0 is the distance between the face of the column and the first perimeter of shear reinforcement (a mean value was calculated for the cases where this distance was not constant); ρ_w is the punching reinforcement ratio; V_{test} is the observed failure load of the connection.